ISSN 1070-3284, Russian Journal of Coordination Chemistry, 2023, Vol. 49, No. 11, pp. 735–742. © Pleiades Publishing, Ltd., 2023.
Russian Text © The Author(s), 2023, published in Koordinatsionnaya Khimiya, 2023, Vol. 49, No. 11, pp. 711–718.

Structure and Magnetic Properties of the Single Crystal of the Liquid-Crystalline Cu(II) Complex with β-Enaminoketone

O. A. Turanova[a, *], **A. T. Gubaidullin**[b], **A. A. Sukhanov**[a], **E. N. Frolova**[a], **V. N. Kovganko**[c], **A. F. Saifina**[b], **and A. N. Turanov**[a]

[a] *Zavoisky Physical Technical Institute, Federal Research Center, Kazan Scientific Center, Russian Academy of Sciences, Kazan, Russia*
[b] *Arbuzov Institute of Organic and Physical Chemistry, Federal Research Center, Kazan Scientific Center, Russian Academy of Sciences, Kazan, Russia*
[c] *Belarusian State Technological University, Minsk, Belarus*
**e-mail: lightur@mail.ru*

Received December 14, 2022; revised April 6, 2023; accepted April 10, 2023

Abstract—The structure and magnetic properties of the single crystal of bis{1-[4-(4-pentyloxybenzoyloxy)phenyl]-1-amino-3-pentylprop-1-en-3-onate}copper(II), which shows nematic mesomorphism, were studied by X-ray diffraction and electron spin resonance spectroscopy.

Keywords: X-ray diffraction analysis, electron spin resonance, liquid crystal, enamonoketone, Cu(II)

DOI: 10.1134/S1070328423600614

INTRODUCTION

Metallomesogens are liquid crystals (LCs) formed by coordination compounds. The presence of a metal ion gives rise to interesting combinations of physical properties typical of both metal compounds (electrical, magnetic, and optical properties) and liquid crystals (combination of fluidity and anisotropy). The ability of metallomesogens to self-assemble into supramolecular structures and respond to weak external stimuli makes them promising materials for electronics. Metallomesogens are used as multifunctional materials, because they can combine the liquid-crystalline state with photo- and electroluminescence, which makes them useful for optoelectronics, power engineering, and biomedicine [1, 2]. An important task of the molecular design of metallomesogens is to elucidate the relationship between the structure and liquid-crystalline properties. It is necessary to take account of the effect of metal ion on the geometry of the chelate unit, which determines not only physical, but also liquid-crystalline properties [3]. The most useful method for structure determination is X-ray diffraction analysis, because the crystals possess strictly periodic structure and act as a diffraction grating for X-rays. Also, reliable data on the structure of the local environment of the metal ion in the complex and on the conformation of the chelate unit can be gained by electron spin resonance (ESR). A combination of X-ray diffraction with ESR spectroscopy provides the most accurate and reliable structural information about coordination compounds.

Previously, a homologous series (C_3H_7–C_9H_{19}) of liquid-crystalline bis{1-[4-(4-alkyloxybenzoyloxy)-phenyl]-1-amino-3-pentylprop-1-en-3-onate}copper(II) complexes has been prepared [4]. It was shown that the presence of the ester group in ligands of this type results in decreasing melting point and increasing width of the nematic mesophase compared to their biphenyl analogues. Amorphous powders, oriented melts, and solutions of these compounds in toluene ($g_x = g_y = 2.039 \pm 0.005$; $g_z = 2.205 \pm 0.005$; $A_x = A_y = 40 \pm 5$ MHz; $A_z = 490 \pm 10$ MHz) were investigated by ESR. The chelate unit of these complexes was found to have a square planar structure, which enables the formation of a liquid-crystalline texture [5]. In this study, the structure of bis{1-[4-(4-pentyloxybenzoyloxy)-phenyl]-1-amino-3-pentylprop-1-en-3-onate}copper(II) (**I**), demonstrating nematic isomorphism (Cr 128 N 209 I), was investigated by ESR spectroscopy and X-ray diffraction. The structure and ESR parameters of single-crystalline complex **I** are presented. Copper(II) complex **I** is shown in Scheme 1.

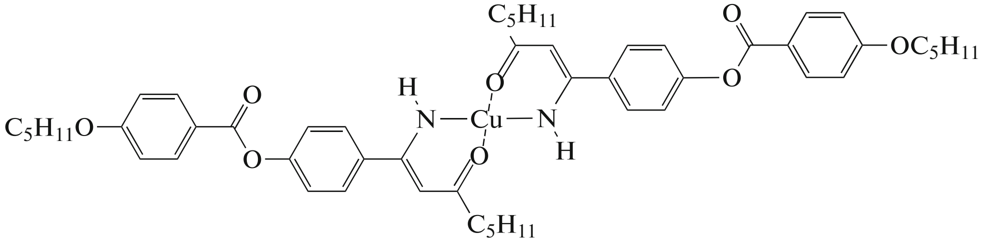

Scheme 1.

EXPERIMENTAL

Complex **I** was prepared by a reported procedure [4]. A single crystal of the complex was prepared by slow evaporation of a solution of the complex in a CH_2Cl_2 : (1,4-dioxane) : EtOH solvent mixture (1 : 2 : 1) for 14 days. The plate-like light green crystals were collected on a filter, washed with EtOH, and air dried.

For $C_{52}H_{64}N_2O_8Cu$			
Calcd., %	C, 68.72	H, 7.05	N, 3.08
Found, %	C, 68.68	H, 7.00	N, 3.02

Single crystal X-ray diffraction study of I was carried out on a Bruker Smart Apex II CCD automated X-ray diffractometer (MoK_α, graphite monochromator, $\lambda = 0.71073$ Å, ω-scan mode) at 296 K. Data collection and editing and refinement of unit cell parameters were performed using the APEX2 program [6]. The structures were solved by the direct method and refined by the least-squares method, first in the isotropic and then in the anisotropic approximation (for all nonhydrogen atoms) using the SHELXL program [7]. The coordinates of hydroxyl hydrogen atoms were revealed from electron density difference plots; the coordinates of other hydrogen atoms were established using stereochemical criteria and refined in the corresponding riding models. All calculations were carried out on a PC using the WinGX software [8]. Analysis of the intermolecular interactions was performed and the drawings were made using the PLATON [9] and Mercury [10] programs. The crystallographic characteristics and X-ray experiment and structure refinement details are summarized in Table 1.

The full set of X-ray diffraction parameters for complex **I** is deposited with the Cambridge Crystallographic Data Centre (CCDC no. 2211696; www.ccdc.cam.ac.uk/data_request/cif).

ESR spectra were recorded in the X range at a temperature of 300 K on an EMX/plus Bruker spectrometer. The angular dependence was studied using an ER 218PG1 Bruker programmable goniometer. The spectra were analyzed using the Easyspin program package [11].

RESULTS AND DISCUSSION

According to X-ray diffraction data, complex **I** forms plate-like crystals (Fig. 1a). The structure was solved and refined in the triclinic space group $P\bar{1}$. Two molecules of the complex are located in special positions (centers of symmetry) of the triclinic unit cell, so that two halves of the molecules are independent. The complexes have a square planar structure of the chelate unit, which is responsible for their mesomorphic properties (Fig. 1b). The copper ions are coordinated by two nitrogen atoms and two oxygen atoms of two ligands, i.e., the donor environment is N(2)O(2); the distances from copper atoms to the oxygen and nitrogen atoms in molecules A and B are as follows: N(1A)–Cu(1A) 1.894(4); O(3A)–Cu(1A) 1.914(3); N(1B)–Cu(1B) 1.878(4); O(3B)Cu(1B) 1.932(3) Å.

The geometries of the two molecular complexes are markedly dissimilar, first of all, this is related to different rotation angles of the aromatic rings and conformations of alkyl substituents. A conventional superimposition of two molecules of the complex is shown in Fig. 2.

The key structure-forming function in the crystals of compound **I** is performed by C–H...O type nonclassical hydrogen bonds and C–H...π electronic contacts involving the aromatic moieties of the molecules; the contact parameters are given in Table 2. Note that the NH groups of the complex molecules do not participate in any interactions, apparently, due to steric hindrances. Owing to the centrosymmetrical position of Cu(II) complex molecules in the crystal, all the existing intermolecular interactions are identical on both sides of the elongated molecule; hence, multiple C–H...π contacts of aromatic moieties (H...Cg (center of the ring) distances are in the 2.60–3.00 Å range) (Fig. 3a) bind the molecules to one another to form an infinite chain along the 0*a* crystallographic axis (Fig. 3a). The C–H...O type hydrogen bonds between molecules connect the chains into two-dimensional supramolecular motifs, that is, layers of H-bonded molecules arranged parallel to the 0*ab* crystallographic plane (Fig. 3b).

Generally, the packing of molecules in the crystal of complex **I** represents a parallel arrangement of the above supramolecular 2D structures along the 0*c* crys-

Table 1. Crystallographic characteristics and structure refinement details for complex **I**

Parameter	Value
Molecular formula	$C_{52}H_{64}N_2O_8Cu$
Crystal shape	Prismatic
M	908.59
Temperature, K	296(2)
System	Triclinic
Space group	$P\bar{1}$
Crystal size	0.02 × 0.33 × 0.70 mm
Z, Z'	2, 1
a, Å	9.789(3)
b, Å	11.247(4)
c, Å	22.412(8)
α, deg	81.381(4)
β, deg	88.377(4)
γ, deg	84.890(5)
V, Å^3	2429.7(14)
$F(000)$	966
ρ(calcd.), g/cm^3	1.242
μ, mm^{-1}	5.04
Range of θ angles, deg	$1.930 \leq \theta \leq 27.946$
Number of measured reflections (R_{int})	19346 (0.0535)
Number of unique reflections	10594
Number of reflections with $I > 2\sigma(I)$	4393
Number of refined parameters	555/12
R_1/wR_2 (reflections with $I > 2\sigma(I)$)	0.0729/0.1758
R_1/wR_2 (for all reflections)	0.1791/0.2271
GOOF on F^2	0.969
Residual electron density (max/min), (e Å^{-3})	0.707/–0.520

tallographic axis (Fig. 3c). With this packing, a high density is not attained: the calculated Kitaigorodsky packing index is 0.641, which is lower than the values typical of organic crystals (0.65–0.75), although the total size of voids in the crystal potentially accessible to a solvent is not very high, being 65.9 Å^3. It is noteworthy that two independent molecules, which markedly differ in the geometry, form separate layers in the crystal (Fig. 4), while the largest-area face of the plate-like single crystal coincides with the (001) crystallographic plane (Fig. 1a), which accommodates the terminal groups of the alkyl chains. Thus, this surface should exhibit noticeable hydrophobic properties, while the crystal itself should possess a marked anisotropy of physical properties.

The substantial anisotropy of magnetic properties of the crystals was evidenced by ESR data. Figure 5 shows the angular dependences of the experimental spectra for two crystal orientations at 300 K. Analysis of the integrated intensity of the ESR spectra provides the conclusion that easy axis magnetic anisotropy exists in the crystal, parallel to the 0*ab* plane of the single crystal unit cell. When this axis is arranged along the magnetic field of the spectrometer, not only the spectrum “collapses” to one line, but also the integrated intensity of the signal increases (Fig. 5c).

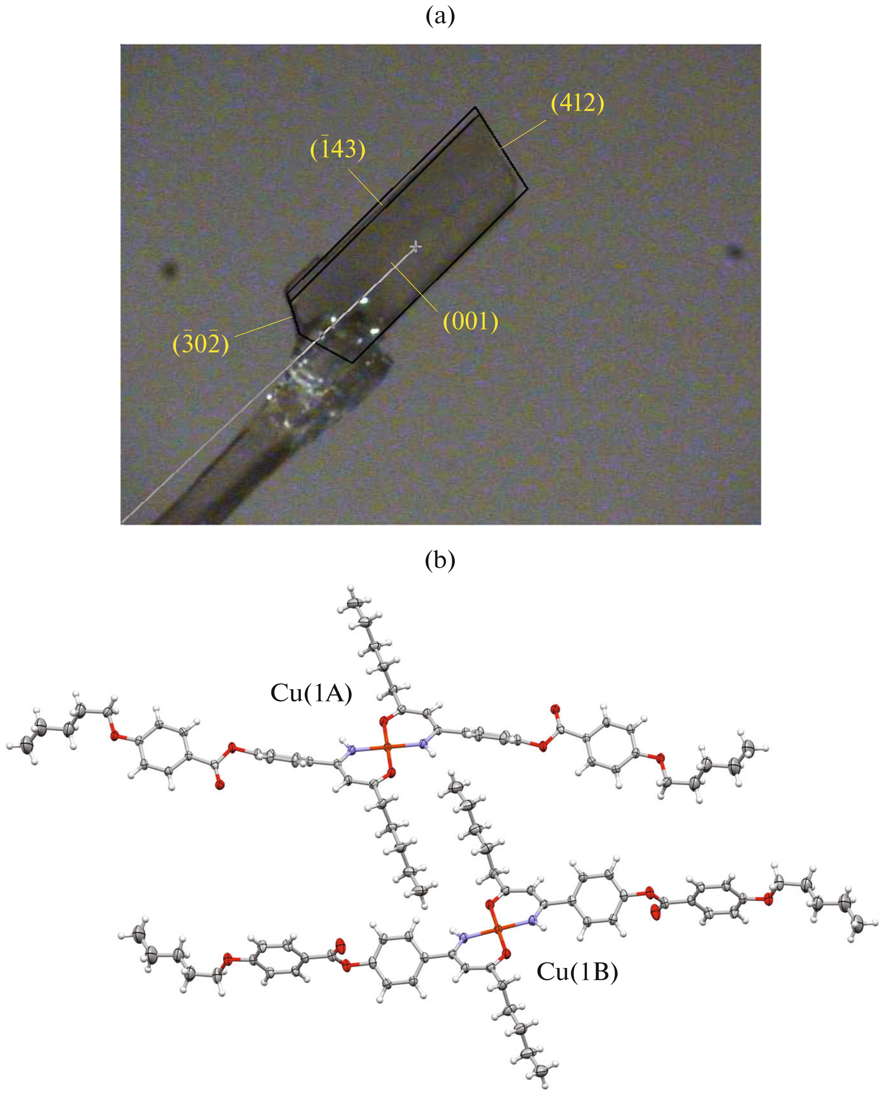

Fig. 1. (a) Photograph of the single crystal of complex **I** and Miller indices of the main crystal faces; (b) geometry of the molecular complexes in the crystal. The nonhydrogen atoms are represented by the thermal probability ellipsoids ($p = 30\%$); hydrogen atoms are shown as spheres of an arbitrary radius.

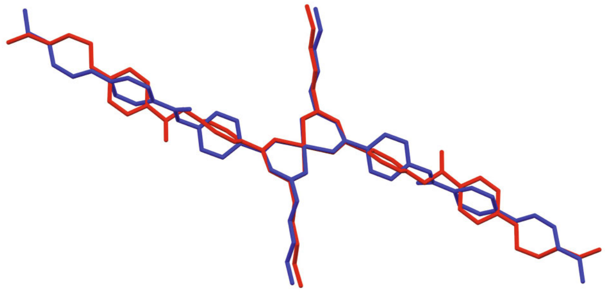

Fig. 2. Conventional superimposition of two molecules of complex **I** (the two symmetrically independent molecules are shown in different colors; the hydrogen atoms are not shown).

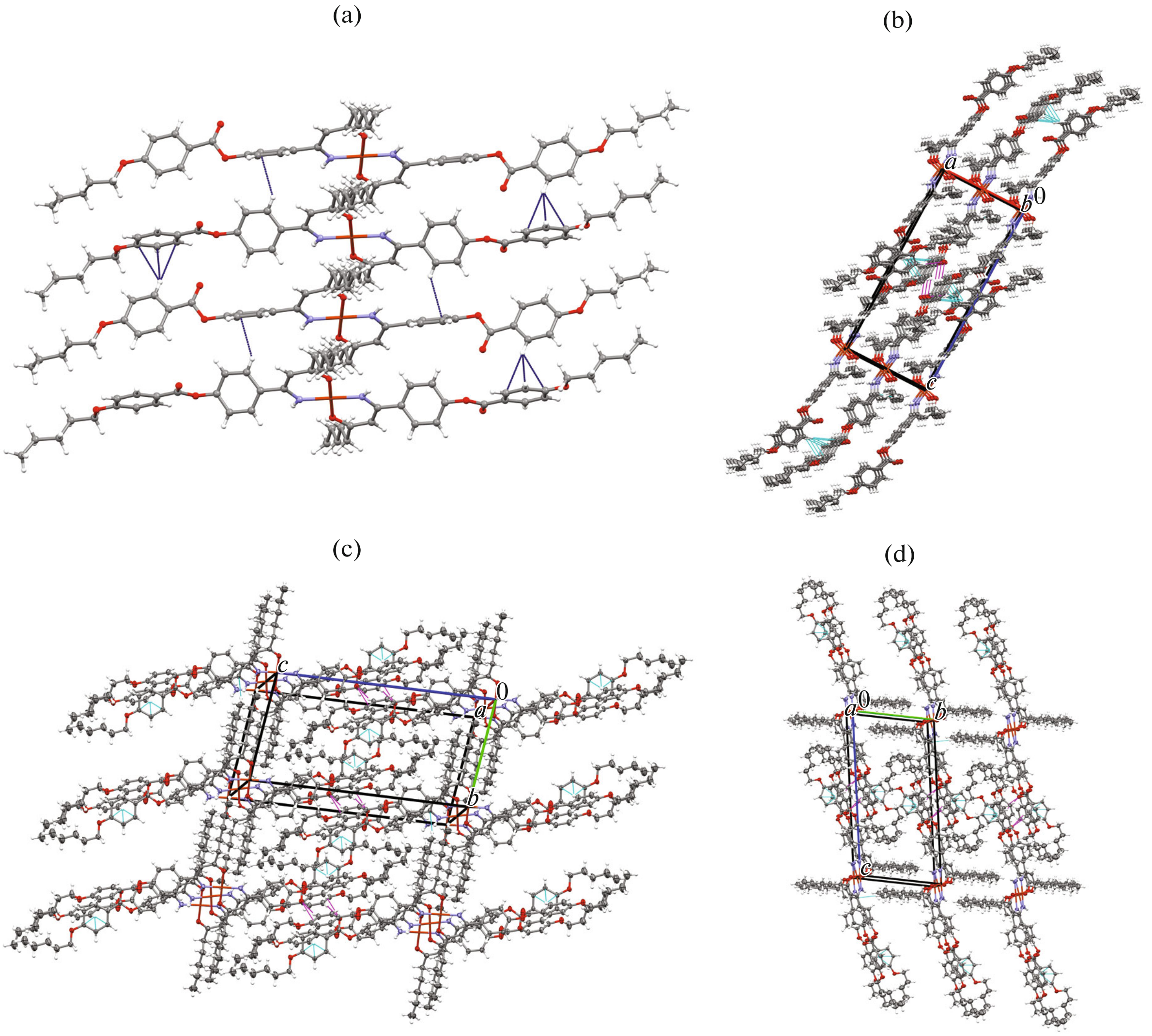

Fig. 3. Several projections of the system of intermolecular C—H...O hydrogen bonds (lilac dashed lines) and C—H...π contacts (blue and light blue dashed lines) in the Cu(II) crystal: a view along the (a, c) 0*a* crystallographic axis and (b) 0*b* crystallographic axis.

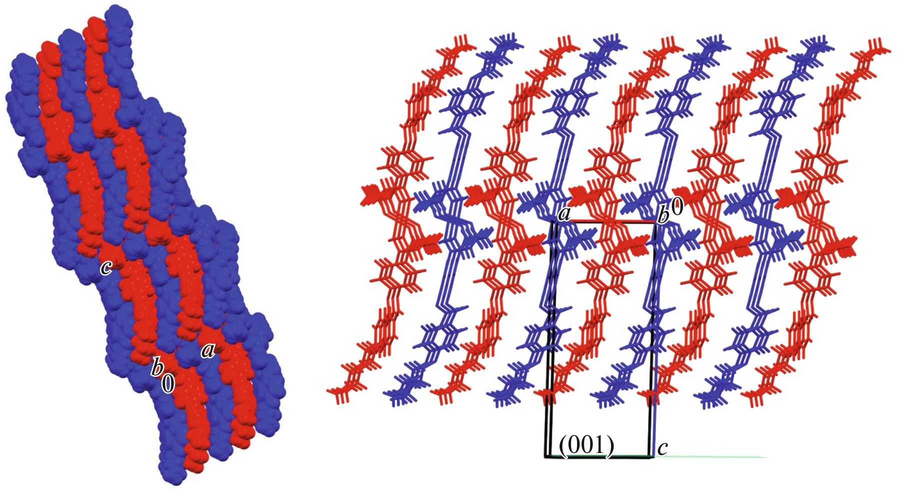

Fig. 4. Two projections of the packing of moleculles of **I** in the crystal; two independent molecules are shown in different colors. The (001) plane is shown in green.

Table 2. Geometric parameters of intermolecular contacts in the crystals of complex **I***

<table>
<tr><th rowspan="2">D–H···A angle</th><th colspan="3">Distance, Å</th><th rowspan="2">Angle D–H···A, deg</th></tr>
<tr><th>D–H</th><th>H···A</th><th>D···A</th></tr>
<tr><td>C(18B)–H(18B)···O(15A)^{i}</td><td>0.93</td><td>2.59</td><td>3.493(6)</td><td>165</td></tr>
<tr><td>C(21A)–H(210)···O(15A)^{ii}</td><td>0.93</td><td>2.57</td><td>3.406(6)</td><td>149</td></tr>
<tr><th rowspan="2">C–H···π contact (Cg is the center of gravity of the ring)</th><th colspan="2">Distance, Å</th><th colspan="2" rowspan="2">C–H...Cg angle, deg</th></tr>
<tr><th>H...Cg</th><th>C...Cg</th></tr>
<tr><td>C(14A)–H(14A)···Cg(C(9B)–C(14B))^{iii}</td><td>2.76</td><td>2.72</td><td colspan="2">155</td></tr>
<tr><td>C(21B)–H(211)···Cg(C(16A)–C(21A))^{iv}</td><td>2.60</td><td>2.58</td><td colspan="2">153</td></tr>
</table>

* Symmetry codes: ^{i} $1 - x, 1 - y, 1 - z$; ^{ii} $1 - x, -y, 1 - z$; ^{iii} $x, -1 + y, z$; ^{iv} $-1 + x, 1 + y, z$.

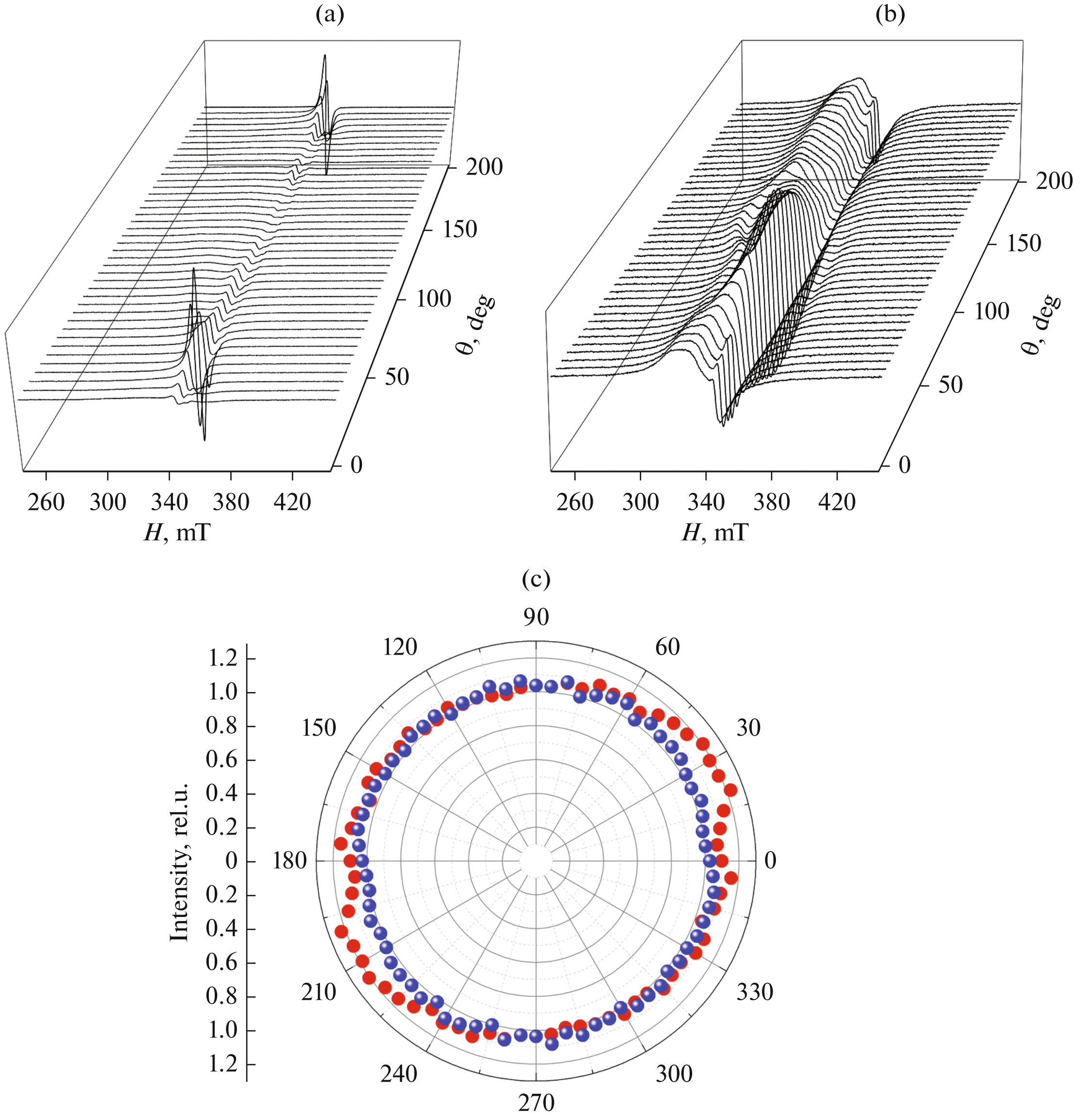

Fig. 5. Angular dependences of the ESR spectra of the single crystal for the magnetic field *H* (a) oriented parallel to the 0*ab* crystallographic plane and (b) in the perpendicular plane; (c) diagram of the angular dependence of the integral intensity of the spectra for both crystal orientations.

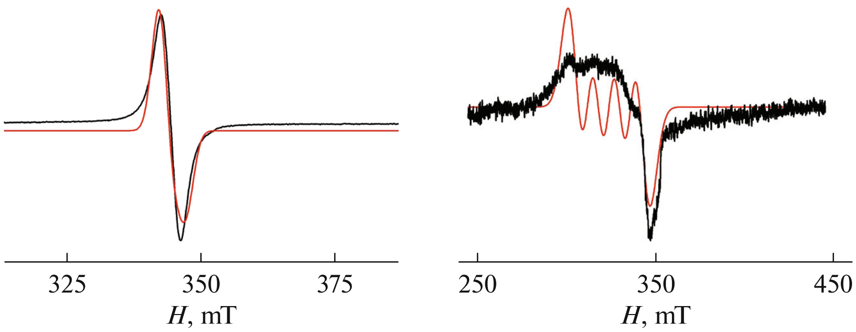

Fig. 6. Experimental (black lines) and simulated (red lines) ESR spectra for two mutually perpendicular orientations of the crystal for the magnetic field H oriented parallel to the 0ab crystallographic plan.

The observed angular dependences of the ESR line shape can be interpreted in terms of the model of weakly coupled spin $S = 1/2$ chains with allowance for the uniform Dzyaloshinskii–Moriya interaction and anisotropic Zeeman interaction [12, 13].

The dominant exchange interaction parameter J of closely located (4.89 Å) copper ions along the 0a axis appears to be not higher than ~2.8 K [14, 15]. The exchange interaction J' between ions located in different chains should be much lower: $J'/J < 0.01$ [13, 16]. Unfortunately, simulation of the spectra does not allow unambiguous determination of exchange interaction parameters. For more in-depth understanding of the properties of the system, measurements of temperature dependences of the magnetic susceptibility of the crystals are required.

Nevertheless, fitting of the experimental and simulated spectra resulted in determination of the parameters characterizing the symmetry of the copper local environment in the crystal packing: $g_x = g_y = 2.045 \pm 0.005$, $g_z = 2.180 \pm 0.005$, $A_x = A_y = 30 \pm 5$ MHz, $A_z = 360 \pm 10$ MHz (Fig. 6). These values are characteristic of a copper ion in the square planar environment [5, 17]. The obtained g-factor anisotropy for the crystal amounting to 0.135 is in good agreement with $\Delta g = 0.130–0.142$ found previously for powders of these compounds [5]. The decrease in A_z for the single crystal compared to that in disordered media may be attributable to the deviation of the complex geometry from planarity. Unfortunately, because of ESR line broadening caused by the dipole–dipole and exchange interactions in the single crystal, it was yet impossible to reliably separate the two types of copper centers identified by X-ray diffraction.

Thus, the structure of bis{1-[4-(4-pentyloxybenzoyloxy)phenyl]-1-amino-3-pentylprop-1-en-3-onate-copper(II) was studied by X-ray diffraction, its crystallographic characteristics were described, and the magnetic parameters of the Cu(II) local environment were determined on the basis of the ESR spectra.

FUNDING

This study was performed within the state assignment for the Federal Research Center, Kazan Scientific Center, Russian Academy of Sciences.

CONFLICT OF INTEREST

The author of this work declares that they has no conflicts of interest.

REFERENCES

1. *Metallomesogens: Synthesis, Properties, and Applications*, Serrano J.L., Ed., New York: Wiley VCH, 1996.
2. Cuerva, C., Cano, M., and Lodeiro, C., *Chem. Rev.*, 2021, vol. 121, no. 20, p. 12966. https://doi.org/10.1021/acs.chemrev.1c00011
3. Torroba, J. and Bruce, D.W., *Comprehensive Inorganic Chemistry II*, Reedijk J. and Poeppelmeier, K., Eds., Elsevier, 2013, vol. 8, p. 837. https://doi.org/10.1016/B978-0-08-097774-4.00824-X
4. Kauhanka, U.M. and Kauhanka, M.M., *Liq. Cryst.*, 2006, vol. 33, no. 2, p. 213. https://doi.org/10.1080/02678290500429638
5. Kovganko, V.N., Kovganko, N.N., Turanova, O.A., et al., *Russ. J. Coord. Chem.*, 2010, vol. 36, no. 4, p. 289.
6. *APEX2 (version 2.1), SAINTPlus. Data Reduction and Correction Program (version 7.31A)*, Bruker Advanced X-ray Solutions. Madison: Bruker AXS Inc., 2006.
7. Sheldrick, G.M., *Acta Crystallogr., Sect. C: Struct. Chem.*, 2015, vol. 71, p. 3. https://doi.org/10.1107/S2053229614024218
8. Farrugia, L.J., *J. Appl. Crystallogr.*, 1999, vol. 32, p. 837. https://doi.org/10.1107/S0021889899006020
9. Spek, A.L., *J. Appl. Crystallogr.*, 2003, vol. 36, p. 7. https://doi.org/10.1107/S0021889802022112

10. Macrae, C.F., Edgington, P.R., McCabe, P., et al., *J. Appl. Crystallogr.*, 2006, vol. 39, p. 453. https://doi.org/10.1107/S002188980600731X
11. Stoll, S. and Schweiger, A., *J. Magn. Reson.*, 2006, vol. 178, no. 1, p. 42. https://doi.org/10.1016/j.jmr.2005.08.013
12. Zakharov, D., Krug von Nidda, H.-A., Eremin, M., et al., *Quantum Magnetism*, Bernard, B., Imry, Y., Sawatzky, G., and Stamp, P.C.E., Eds., Springer Science, Business Media B.V., 2008, p. 193. https://doi.org/10.1007/978-1-4020-8512-3_14
13. Hoffmann, S.K., Hilczer, W., and Goslar, J., *Appl. Magn. Reson.*, 1994, vol. 7, p. 289. https://doi.org/10.1007/BF03162617
14. Tarasenko, R., Orendacova, A., Cizmar, E., et al., *Phys. Rev. B*, 2013, vol. 87, p. 174401. https://doi.org/10.1103/PhysRevB.87.174401
15. Voronkova, V., Galeev, R., Korobchenko, L., et al., *Appl. Magn. Reson.*, 2005, vol. 28, p. 297. https://doi.org/10.1007/BF03166763
16. Sengupta, P., Batista, C.D., McDonald, R.D., et al., *Phys. Rev. B*, 2009, vol. 79, p. 060409. https://doi.org/10.1103/PhysRevB.79.060409
17. Yokoi, H. and Addison, A.W., *Inorg. Chem.*, 1977, vol. 16, no. 6, p. 1341. https://doi.org/10.1021/ic50172a018

Translated by Z. Svitanko